

1 **MANUSCRIPT**

2 **Molecular characterization of *EZH2*-mutant patients with**

3 **myelodysplastic/myeloproliferative neoplasms**

4 Jenny Rinke¹, Jörg P. Müller², Markus F. Blaess³, Andrew Chase^{4,5}, Manja
5 Meggendorfer⁶, Vivien Schäfer¹, Nils Winkelmann¹, Claudia Haferlach⁶, Nicholas
6 C.P. Cross^{4,5}, Andreas Hochhaus¹, Thomas Ernst¹

7 ¹ Abteilung Hämatologie und Internistische Onkologie, Klinik für Innere Medizin
8 II, Universitätsklinikum Jena, Jena, Germany

9 ² Institut für Molekulare Zellbiologie, Center for Molecular Biomedicine,
10 Universitätsklinikum Jena, Jena, Germany

11 ³ Klinik für Anästhesiologie und Intensivmedizin, Universitätsklinikum Jena,
12 Jena, Germany

13 ⁴ National Genetics Reference Laboratory (Wessex), Salisbury District Hospital,
14 Salisbury, UK

15 ⁵ Faculty of Medicine, University of Southampton, Southampton, UK

16 ⁶ MLL Münchner Leukämielabor, Munich, Germany

17

18 Correspondence: PD Dr. Thomas Ernst, Abteilung Hämatologie und Internistische
19 Onkologie, Klinik für Innere Medizin II, Universitätsklinikum Jena, Am Klinikum 1,
20 07740 Jena, Germany; Phone: +49 3641 9324563; Fax: +49 3641 9324202; E-Mail:
21 thomas.ernst@med.uni-jena.de

22

23 **Keywords:** *EZH2*, mutation, CMML, MDS/MPN, *ETS1*, target genes

24

25 **Running Title:** *EZH2* dysregulation in MDS/MPN

26

27 **Word count:**

28

29 **Abstract**

30 Mutations in the epigenetic regulator gene *EZH2* are frequently observed in patients
31 with myelodysplastic/myeloproliferative neoplasms (MDS/MPN; 10-13%) and are
32 associated with a poor outcome. To gain more insight into *EZH2* pathology we
33 sought to genetically characterize a cohort of 41 *EZH2*-mutated MDS/MPN patients
34 using targeted deep next generation sequencing (NGS), colony forming progenitor
35 assays and transcriptome analysis. Stable shRNA-mediated downregulation of *EZH2*
36 was performed in MDS derived F-36P, MOLM-13 and OCI-M2 cells to study *EZH2*
37 specific changes. Targeted NGS revealed a complex pattern of mutations with a total
38 of 190 individual mutations. *EZH2* mutations frequently co-occur with *TET2* (58%),
39 *RUNX1* (40%) and *ASXL1* (34%) mutations. Colony assays indicated *EZH2*
40 mutations to be mostly early events in leukemogenesis and showed a complex
41 mutational hierarchy. Gene expression data revealed a number of differently
42 expressed genes between *EZH2*-wild type and mutant patients including known
43 *EZH2* targets. Comparison of patient transcriptome to *EZH2* downregulated cell line
44 data revealed several genes as novel *EZH2* targets, showing opposite as well as
45 unidirectional regulation between cell lines and patients. Some genes, such as
46 *CXXC5*, *ETS1* and *VAV3* have previously been implied to play a role in
47 leukemogenesis. Their precise role in MDS/MPN needs to be further investigated.

48

49

50

51

52

53

54

55 **Introduction**

56 Discoveries like *BCR-ABL1* in chronic myeloid leukemia (CML)¹ and *JAK2-V617F* in
57 polycythemia vera (PV)² have shown that single molecular aberrations can bring
58 about a better understanding of a disease entity and aid classification and
59 treatment.^{3,4}

60 However, in recent years, through advances in sequencing technology, particularly
61 next generation sequencing (NGS), the ongoing effort to better define the molecular
62 background of myeloid malignancies has revealed a perhaps unexpected complexity.

63 A large number of somatic mutations affecting multiple pathways have been identified
64 with varying frequencies and combinations that overlap the different disease entities.⁵

65 Originally aberrations were discovered in genes that confer a growth advantage by
66 altering signaling pathways and expression of key transcriptional targets.⁶ Over time
67 additional pathways such as epigenetic modification, RNA splicing, and as recently
68 discovered the cohesin complex, in particular *STAG2*, were found to be involved in
69 myeloid leukemogenesis.^{5,7,8} The task at hand is to unravel these heterogeneous
70 molecular patterns and hierarchies, to study their effects on disease phenotype and
71 ultimately to identify new therapeutic targets. Epigenetic targeted therapy is of
72 particular interest because epigenetic changes – unlike somatic gene mutations – are
73 potentially reversible and offer promising therapeutic alternatives even in elderly
74 patients.⁹

75 This study focuses on myeloproliferative/myelodysplastic neoplasms (MDS/MPN) in
76 adults, as this overlap category encompasses both the dysplastic and the
77 hyperproliferative features seen in other myeloid malignancies. Chronic
78 myelomonocytic leukemia (CMML) is the most common entity in this category with a
79 heterogeneous genetic background that is reflected in the diverse clinical and
80 pathological features of this disease. Other diseases in the MDS/MPN category show

81 a similar complexity and include *BCR-ABL1*-negative atypical chronic myeloid
82 leukemia (aCML), MDS/MPN, unclassifiable (MDS/MPN-U) and juvenile
83 myelomonocytic leukemia (JMML).³

84 Amongst the most frequently mutated signaling genes in MDS/MPN are *CBL* (8-
85 20%), *KRAS* (7-11%), *NRAS* (4-30%) and *SETBP1* (6-25%). Aberrations of
86 components of the RNA splicing machinery are common, most frequently involving
87 *SRSF2* with mutations detectable in 36-46% of CMML patients and less frequently
88 involving *U2AF35* (5-15%) and *ZRSR2* (8-10%). *RUNX1* which encodes a
89 transcription factor involved in cell growth, survival and differentiation is mutated in 6-
90 20% of MDS/MPN cases. Thirty to 60% of patients show *TET2* mutations and less
91 than 10% *DNMT3A* and *IDH1/2* mutations, all of which impair DNA methylation.
92 Other epigenetic changes affecting histone modifications are frequently detected in
93 *ASXL1* (20-44%) and *EZH2* (6-13%).⁵

94 *EZH2* is an epigenetic regulator gene encoding the catalytic subunit of the polycomb
95 repressive complex 2 (PRC2), a histone H3 lysine 27 (H3K27) methyltransferase.
96 Gain-of-function mutations in this gene have previously been observed in prostate,
97 breast and bladder cancer amongst others.¹⁰ Remarkably, loss-of-function mutations
98 have been detected in myeloid malignancies, highlighting the ambiguous role of
99 *EZH2* in cancer. Such mutations are associated with poor overall and progression-
100 free survival and occur most frequently in the MDS/MPN category (10-13%).¹¹

101 In light of these findings we aimed to genetically characterize a cohort of 41 *EZH2*-
102 mutated MDS/MPN patients to investigate mutational patterns associated with *EZH2*.
103 To better understand the complex clonal hierarchies of detected mutations, colony
104 assays were carried out. Additionally, to investigate the effect of loss-of-function
105 *EZH2* mutations on gene expression we carried out whole transcriptome analysis on
106 a subset of our patient cohort compared to *EZH2*-wild type MDS/MPN patients. To

107 identify specific *EZH2* targets, we compared results to cell lines F-36P, MOLM-13
108 and OCI-M2, where suppression of *EZH2* translation was achieved by stable
109 transduction of *EZH2*-targeting shRNAs.

110 **Methods and Patients**

111 *Patients*

112 Bone marrow (BM) samples were collected from 41 *EZH2*-mutation positive
113 MDS/MPN patients (CMML, n = 25; aCML, n = 11; MDS/MPN-U, n = 5; male, n =
114 25). Patients were classified according to the 2008 WHO classification of myeloid
115 neoplasms and acute leukemia.³ Bone marrow samples of a cohort of 12 *EZH2*-
116 wildtype MDS/MPN patients (A - L; male, n = 9) were used as a control group.
117 Clinical information is given in Supplemental Table 1. The study has been approved
118 by the institutional ethics committee and written informed consent was provided
119 according to the Declaration of Helsinki.

120 *Sample Preparation*

121 Total BM leukocytes were isolated after erythrocyte lysis according to standard
122 protocols. Leukocyte RNA extraction was performed using TRIzol® reagent, as
123 described previously.¹² Genomic DNA from leukocytes was extracted using the
124 QIAamp DNA Mini Kit (Qiagen, Hilden, Germany) according to the manufacturer's
125 guidelines. Mononuclear cells were isolated according to standard procedures using
126 Ficoll density gradient centrifugation, and CD34+ selected by MACS® separation with
127 the CD34 MicroBead Kit (Miltenyi Biotec, Bergisch Gladbach, Germany) according to
128 manufacturer's instructions.

129 *Next-generation sequencing (NGS)*

130 NGS, including data analysis was performed for 30 leukemia-associated target genes
131 on the 454 GS Junior platform with 454 GS Junior Titanium chemistry for amplicon
132 sequencing (Roche Diagnostics, Basel, Switzerland) as previously described.^{13,14} In

133 total, 231 amplicons were prepared for each sample and processed in a single NGS
134 run. Mutations with a frequency >15% were confirmed using Sanger Sequencing with
135 standard techniques on an ABI 3500 Genetic Analyzer (Thermo Fisher Scientific,
136 Waltham, MA, USA) as described previously.¹⁴ DNA-sequencing raw data is
137 available on reasonable request.

138 *Colony Assays and Sanger Sequencing*

139 Cryoconserved CD34+ cells of patients #24, 37, 40 and 41 were plated and
140 processed for analysis by colony assay as previously described.¹⁵ To check the
141 specific mutational status of individual colonies, Sanger sequencing of PCR products
142 covering the relevant genetic regions was performed according to standard
143 techniques.¹⁴ Mutational analysis was performed using the Mutation Surveyor
144 Software (SoftGenetics, State College, PA, USA). A dropping factor (drop in height of
145 the normal peak at the position of the mutation relative to the neighboring peaks) of
146 <30% was considered indicative of wild type, a dropping factor between 30% and
147 70% was considered to be a heterozygous mutation and a factor >70% was
148 considered to be homozygous.

149 *Stable shRNA-mediated downregulation of EZH2*

150 Two shRNA encoding oligonucleotides targeting *EZH2* (shEZH2_1: 5' -
151 GAGAGATTATTTCTCAAGATG- 3'; shEZH2_2: 5' -TGGAAAGAACGGAAATCTTAA
152 -3'), or a non-targeting control shRNA (Sigma-Aldrich, St. Louis, MO, USA) were
153 inserted between AgeI and EcoRI restriction sites into plasmid pLKO.1 (Sigma).
154 Expression constructs were transduced and selected in cell lines F-36P (ACC-543),
155 MOLM-13 (ACC-554) and OCI-M2 (ACC-619), purchased from The Leibniz Institute
156 DSMZ - German Collection of Microorganisms and Cell Cultures GmbH, as described
157 previously¹⁶ and tested for mycoplasma contamination. Growth curves of cell lines

158 were generated using the CellTiter-Glo cell viability assay (PROMEGA, Fitchburg,
159 WI, USA), according to manufacturer instructions.

160 *Whole transcriptome analysis and qRT-PCR*

161 Total RNA (200 ng) of 24 MDS/MPN BM leukocyte samples (n = 12 *EZH2*-mutated
162 and wild type cases, respectively) as well as sh*EZH2*_1 and sh*EZH2*_2
163 downregulated F-36P, MOLM-13 and OCI-M2 cell lines and respective control cells
164 transduced with non-targeting shRNA (4 each, collected at 4 time points) were
165 processed and analyzed as previously described.¹⁷ Control probe quality check,
166 background subtraction, signal averaging and data analysis were performed using
167 Illumina GenomeStudio-Software v.2011.1 (Illumina, San Diego, CA, USA) and
168 GraphPad Prism v6.01 (GraphPad Software, Inc., San Diego, CA, USA). Expression
169 data obtained from *EZH2*-wild type vs. mutant MDS/MPN patients for genes showing
170 FC values ≥ 2 and signal intensities ≥ 100 , as well as detection p-values < 0.05 in at
171 least one group, were subjected to statistical analysis (Mann-Whitney test) and
172 compared to F-36P, MOLM-13 and OCI-M2 expression data (Student's t-test). RNA-
173 seq data have been deposited in the ArrayExpress database at EMBL-EBI
174 (www.ebi.ac.uk/arrayexpress) under accession number E-MTAB-5766. Results were
175 verified using qRT-PCR according to standard protocols with SYBR-green dye
176 (Roche) and *beta glucuronidase (GUSB)* as a reference gene. Primer sequences are
177 available in Supplemental Table 2.

178 *Western blot analysis*

179 Protein blot analysis was performed for genes showing average expression signals
180 > 100 in cell lines and patients, using primary antibodies against *EZH2* (#3147),
181 histone H3 (#9717), H3K27me3 (#9733), CXXC5 (#84546), *ETS1* (#14069), *VAV3*
182 (#2398), *GAPDH* (#2118) (Cell Signaling Technology, Boston, MA, USA), *FAM133B*
183 (HPA043901) (Atlas Antibodies, Bromma, Sweden) and *STS-1* (ab197027) (Abcam,

184 Cambridge, UK). Protein isolation was carried out using 5×10^6 cells, according to
185 standard procedures using radioimmunoprecipitation assay buffer (RIPA) with
186 standard protease inhibitors and 100 mM sodium-ortho-vanadate. For each sample
187 protein lysates were separated, blotted and blocked as previously described.¹⁸ Blots
188 were incubated with the indicated primary antibodies for 16 h at 4°C. After incubation
189 with respective secondary antibodies, chemiluminescent HRP substrate (Millipore,
190 Billerica, MA, USA) was added. Proteins were visualized with ImageQuant LAS-4000
191 (GE Healthcare, Chicago, IL, USA) and quantified using ImageJ (National Institute of
192 Health, Bethesda, MD, USA).

193 **Results**

194 *Cooperating mutations in leukemia-associated genes in 41 EZH2-mutated MDS/MPN* 195 *patients*

196 In total 190 individual mutations affecting 19 genes were detected, including 53
197 mutations of *EZH2*. In addition to *EZH2* mutations, 23/41 patients (56%) showed
198 cooperating *TET2* mutations, followed by *RUNX1* (39%), *ASXL1* (34%), *CBL* (24%),
199 *ZRSR2* (20%), *SRSF2* (15%), *NRAS* (15%), *STAG2* (12%) and *SETBP1* (12%),
200 affecting all five aforementioned pathways. The majority of patients with mutations in
201 *TET2*, *RUNX1* and/or *ASXL1* carried frameshift, nonsense or splice site mutations in
202 these genes (83%, 81%, 93%, respectively), which often have severe functional
203 consequences. Multiple mutations in the same gene were most commonly observed
204 in *TET2* with 16/23 (70%) affected patients showing up to three mutations.
205 Approximately 30% of affected patients carried multiple mutations in *EZH2*, *RUNX1*
206 and *CBL* (Fig 1). Detailed DNA-sequencing data is given in Supplemental Table 3. As
207 some mutations were located on the same amplicon biallelic mutations could be
208 distinguished from monoallelic mutations. Biallelic mutations were detected in
209 patients #4 (*CBL*), 13 (*CBL*) and 26 (*TET2*) whilst patients #30 (*RUNX1*) and 40

210 (*EZH2*) carried monoallelic mutations and patient #32 (*RUNX1*) showed overlapping
211 mutations with indistinct allelic origin (Supplemental Fig 1).

212 *Clonal hierarchies of patients #24, 37, 40 and 41*

213 Analysis of 216 individual colonies for mutations detected by NGS revealed various
214 mutational patterns. The detection of clones carrying only *EZH2* mutations in patients
215 #37 and 40 indicates that *EZH2* precedes the acquisition of *SETBP1* mutations,
216 followed by mutations of *NRAS* and *CBL* respectively (Figs 2A, 2B). In patient #37
217 the low-level *KRAS*, *RUNX1*, *STAG2* and *ZRSR2* mutations previously detected by
218 NGS were not found in the analyzed colonies. The putative evolutionary tree
219 generated for patient #24 also indicates *EZH2* and *SETBP1* mutations to be early
220 events in leukemogenesis (Fig 2C). Overall, a more complex pattern of mutations
221 was detected in this patient, with various subclones, changing from heterozygous to
222 homozygous or wild type states for certain mutations. Interestingly, colony analysis
223 of patient #41 indicates the early acquisition of an *ASXL1* mutation, followed by
224 *EZH2* mutations p.T467Hfs*16 and p.Y579X, respectively (Fig 2D).

225 *Transcriptome analysis of EZH2-wild type and mutant MDS/MPN patients*

226 Initial comparison of transcriptome-wide expression data of *EZH2*-wild type and
227 mutant MDS/MPN patients showed clear differences in overall gene expression,
228 particularly for a number of highly expressed genes, albeit not above 2 FC (Fig 3A).
229 In total 1,375 genes with significant ≥ 2 FC differences between the *EZH2*-wild type
230 and mutant group with average signal intensities above 100 in at least one group
231 were detected. Detailed expression data is given in Supplemental Table 4.
232 Correlation cluster analysis of patient data showed a distinct separation of expression
233 patterns according to *EZH2*-status. Heat map data revealed that most *EZH2*-wild
234 type MDS/MPN patients displayed higher expression levels in the majority of
235 differently expressed genes (Fig 3B). Some known *EZH2*-targets, such as *ADRB2*

236 and the NOTCH- and JAK-STAT pathway genes, *MYC*, *JAK1* and *JAK2*¹⁰ were found
237 to have significantly different expression levels between *EZH2*-mutant and wild type
238 patients (Fig 3C).

239 *Transcriptome analysis of the EZH2 downregulated F-36P, MOLM-13 and OCI-M2*
240 *cell lines*

241 For each cell line we compared transcriptome data of genes that showed significant
242 differences between *EZH2*-wild type and mutant patients as shown above, to gene
243 expression data of sh*EZH2*-downregulated cell lines with the respective control cell
244 line, expressing non targeting control shRNA. All cell lines showed significant
245 differences in expression levels for *CXXC5* and *FAM113B*. For F-36P we found 237
246 genes which showed p-values <0.05 for one or both sh*EZH2* manipulated cell lines.
247 Four of these genes (*PM20D2*, *PRAGMIN*, *RAB3IL1* and *STS-1*) showed ≥ 2 FC,
248 significant differences in both downregulated F-36P lines compared to the control. In
249 MOLM-13 we found 91 genes which showed p-values <0.05 for one or both sh*EZH2*
250 manipulated cell lines. Two genes (*ETS-1* and *VAV3*) showed ≥ 2 FC, significant
251 differences in both downregulated MOLM-13 lines compared to the control. OCI-M2
252 cell lines showed 318 genes with p-values <0.05 for one or both manipulated cell
253 lines. Significant differences in expression for both downregulated OCI-M2 lines were
254 seen in *VAV3*, albeit not ≥ 2 FC. As seen with patient data, a number of previously
255 identified *EZH2* targets^{10,19} showed significant differences in sh*EZH2* downregulated
256 OCI-M2 lines compared to controls. Detailed expression data is given in
257 Supplemental Table 4. Significant differences in *EZH2* expression were only
258 observed in cell lines (Fig 4), as *EZH2* may be expressed but functionally
259 compromised in patients carrying missense mutations. Interestingly, some genes
260 such as *CXXC5*, *ETS-1*, *STS-1* and *VAV3* showed opposite directions of regulation in
261 patients compared to cell models, whilst others such as *FAM113B* and *PRAGMIN*

262 showed regulation in the same direction. Results were confirmed by quantitative real
263 time PCR (qRT-PCR). For cell lines and patients, log₂ array and qRT-PCR data
264 comparing gene expression according to *EZH2* status are shown in Figure 4. Cell
265 viability of cell lines was not affected by EZH2-manipulation (Supplemental Fig 2).

266 *Histone H3 trimethylation and protein expression*

267 Protein blots of all control and shEZH2 cell lines confirmed downregulation of EZH2
268 expression, resulting in reduced H3K27 trimethylation, as a result of impaired EZH2
269 function. Additionally, changes in protein levels of ETS-1, STS-1 and VAV3 were
270 detected for respective cell lines. CXXC5 and FAM113B were on the resolution limit
271 of protein blot analysis, but showed differences <2FC in line with RNA expression
272 data (Fig 5A). Semi-quantified cell line data is shown in optical density charts in
273 Figure 5B. Exemplary patient data showed no EZH2 in patients #27 and 32 as a
274 result of homozygous frameshift mutations (p.K685Rfs*12 and p.K17Sfs*3,
275 respectively). Patients # 24 and 34 carry heterozygous frameshift (p.N263Qfs*8) and
276 nonsense mutations (p.Y292X), respectively. Downregulation of H3K27 trimethylation
277 was observed in EZH2-mutant patients #24, 27, 32 and 34 compared to EZH2-wild
278 type patients D and F though overall EZH2 protein levels were lower (Fig 5C).

279 **Discussion**

280 NGS of *EZH2*-mutant MDS/MPN patients revealed various mutational patterns.
281 *TET2*, *RUNX1* and *ASXL1* were most frequently mutated together with *EZH2*, which
282 is in agreement with previous findings.¹⁹ Interestingly, 39% of patients showed
283 *RUNX1* mutations (Fig 1). This is in line with recent MDS studies showing a
284 significant association of *EZH2* and *RUNX1*.^{20,21} These studies also reported that
285 *EZH2* and *SRSF2* are rarely mutated together. We found *SRSF2* mutations in only
286 15% of our patients. Splicing mutations in *SF3B1* and *U2AF1* did not co-occur with
287 *EZH2* mutations or were present at very low levels (2.4%), respectively (Fig 1). Khan

288 *et al.* have demonstrated that splicing abnormalities are often responsible for loss of
289 *EZH2* function.¹⁹ This may explain why splicing mutations occur rarely in *EZH2*
290 positive patients, as epistasis or synthetic lethality can cause mutual exclusion of
291 certain gene mutations.²² However, heterozygous mutations for multiple genes that
292 regulate PRC2 function can cooperate in leukemic transformations through additive
293 effects.²³

294 Previous findings of *EZH2* mutations in patients with refractory anemia, suggest that
295 *EZH2* mutations are acquired early in leukemogenesis.¹¹ Our analysis of clonal
296 hierarchies confirmed that *EZH2* mutations can indeed be early events, at least in
297 MDS/MPN cases harboring additional *SETBP1* mutations as seen in patients #24, 37
298 and 40. In the latter two acquisition of *NRAS* and *CBL* mutations occurred last (Figs
299 2A, 2B), supporting previous findings that signaling genes are often affected later on
300 in disease progression.²⁴ Results showed a clonal architecture with moderate to
301 frequent branching. Particularly patient #24 displayed a complex pattern of disease
302 evolution (Fig 2C). The progression to homozygous and reversion to wild type states
303 for certain loci can be explained through loss of heterozygosity and reflect the current
304 view of vast genetic diversity in leukemic cells as opposed to the merely linear
305 acquisition of mutations.^{24,25} In support of this mono- and biallelic, as well as
306 overlapping mutations were detected in some patients (Supplemental Fig 1). The
307 clonal hierarchy of patient #41 showed *EZH2* mutations as secondary events,
308 preceded by the acquisition of an *ASXL1* mutation (Fig 2D). A recent study proposed
309 that CMML arises through accumulation of mostly age-related somatic mutations that
310 ultimately convert a skewed myelomonocytic hematopoiesis into leukemia.²⁶ In line
311 with these findings, it has been shown that early clonal dominance, particularly of
312 *TET2* or *ASXL1*-mutant myeloid progenitors is followed by selection of clones
313 carrying secondary lesions during myeloid differentiation.²⁴ Both *TET2* and *ASXL1*

314 have been implicated in age related clonal hematopoiesis (ARCH), thus their role as
315 early key players in the development of CMML is not surprising. In contrast *EZH2*
316 (and *SETBP1*) mutations have not been shown to be involved in ARCH.²⁶ Thus
317 *EZH2* mutations may reflect an alternative mode of MDS/MPN initiation or, in cases
318 where ARCH genes are involved, could provide the growth advantage that is
319 essential for leukemic transformation. In any case the total number of mutated genes
320 seems to be a strong prognostic factor in CMML, indicating that clonal complexity
321 might affect therapy.²⁷ Thus, the delineation of clonal architecture remains of prime
322 importance to ensure therapy is directed at primary lesions.

323 Whole transcriptome analysis of *EZH2*-wild type and mutant MDS/MPN patients
324 showed distinct expression patterns (Fig 3A), suggesting that the *EZH2* mutational
325 status has a global effect on gene expression. Interestingly, *EZH2*-wild type patients
326 show the most upregulation in differently expressed genes, when looking at cluster
327 correlation analysis (Fig 3B). These findings underline the complex role of *EZH2* as
328 an epigenetic regulator that may silence or activate targets by pathway dependent
329 mechanisms. Since multiple mechanisms can affect H3K27me3 (ref. 19) it is not
330 surprising that two patients showed expression patterns distinct from their respective
331 group (Fig 3B). Looking at known *EZH2* targets¹⁰ we found significant differences in
332 *ADRB2*, *JAK1*, *JAK2* and *MYC* between *EZH2*-wild type and mutant patients (Fig
333 3C). Expression levels of genes related to known *EZH2*-targets, such as *HOXA5*,
334 *HOXB5* and *cyclins A1, A2, B1, D2* and *F*, were also affected (Supplemental Table
335 4). However, it is important to note that MDS/MPN patients show vastly
336 heterogeneous genetic lesions, which is reflected in the large number of differently
337 expressed genes and the clinical heterogeneity of these diseases.

338 Therefore *EZH2*-knock-down models were established in sAML cell lines F-36P,
339 MOLM-13 and OCI-M2. We found two genes to be regulated in patients and all cell

340 lines (*CXXC5*, *FAM113B*), and a number of genes that were regulated in patients and
341 at least one cell line, such as *ETS-1*, *STS-1* and *VAV3* (Fig 4). The Wnt-signaling
342 inhibitor *CXXC5* plays a role in myelopoiesis and is a known tumor suppressor
343 candidate, located on 5q31.2, a region recurrently deleted in AML and MDS. Its
344 downregulation has been associated with a better outcome in AML, pointing towards
345 the potential benefits of Wnt-inhibitor treatment.²⁸ ETS proteins are transcription
346 factors that can alter the expression of genes that are involved in various biological
347 processes, such as hematopoiesis, cellular proliferation, differentiation, development
348 and apoptosis.²⁹ ETS1 has long been implied to play a role in hematologic
349 malignancies.^{30,31} Molecular allelokaryotyping of T-cell prolymphocytic leukemia cells
350 revealed recurrent microdeletions targeting *ETS1*.³² Additionally, analyses of low-risk
351 MDS cases found *ETS1* to have tumor suppressor function as the gene was
352 hypermethylated and showed low expression levels, with various ETS1 targets being
353 downregulation as a result.³³ The protein tyrosine phosphatase STS-1 has recently
354 been shown to interact with CBL, regulating myeloid proliferation in human AML1-
355 ETO.³⁴ An interaction between *VAV3* and *EZH2* has previously been revealed for
356 putative homologues in *Saccharomyces cerevisiae*.³⁵ Studies have shown that *VAV3*
357 plays a role in lymphocyte activation and development.³⁶ Interestingly genetic
358 deficiency of *VAV3* delays the progression of *BCR-ABL*-positive lymphoblastic
359 leukemia and increases leukemic cell death making the gene a potential therapeutic
360 target.³⁷

361 The apparent paradox of opposite regulation of some genes between cell lines and
362 patients may occur for a number of reasons. (a) Artificial introduction of *EZH2*
363 dysfunction in sAML cell lines might bring about different effects, compared to *EZH2*
364 mutations in less proliferative MDS cells, whilst still indicating potential targets. (b)
365 *EZH2* expression was overall higher in cell lines compared to patients (Fig 5,

366 Supplemental Table 4). The different levels of EZH2 protein may alter the spectrum
367 of function and modify PRC2 activity, as highlighted by the arbitrary role of *EZH2* as a
368 tumor suppressor and oncogene. (c) The results indicate that *CXXC5*, *ETS-1*, *STS-1*
369 and *VAV3* may not be direct targets of EZH2 but rather fall under the regulatory
370 control of secondary pathways. For example, Viré *et al.*³⁸ have shown that the two
371 epigenetic systems of histone and DNA methylation are connected. Thus DNA
372 methylation could serve as a switch for gene expression, depending on the level of
373 EZH2 activity.

374 In conclusion, we found a spectrum of concurrent and mutually exclusive mutations
375 of *EZH2*-positive MDS/MPN patients similar to molecular patterns observed in MDS.
376 Further studies with larger cohorts will reveal how the mutational landscape affects
377 disease phenotype and response to therapy. *EZH2* mutations seem to be early
378 events in leukemogenesis, particularly when ARCH genes are not involved.
379 Comparison of patient data with *EZH2*-downregulated sAML cell lines revealed
380 *CXXC5*, *FAM113B*, *ETS1*, *STS-1* and *VAV3* expression to be associated with *EZH2*
381 mutational status, amongst other genes with lower expression levels (*PM20D2*,
382 *PRAGMIN*, *RAB3IL1*). Whether these targets are up- or downregulated may depend
383 on initial EZH2 expression and cellular context. At this point the exact pathway,
384 through which EZH2 may exert regulatory control, remains unknown. Nonetheless, to
385 our knowledge this is the first study that has uncovered these genes as EZH2 targets
386 in myeloid malignancies. Further study will reveal their precise role in myeloid
387 leukemogenesis.

388

389

390

391

392 **Acknowledgements**

393 The excellent technical assistance of Mrs. Anja Waldau is gratefully acknowledged.
394 The study was supported by the Deutsche José Carreras Leukämie-Stiftung e.V.
395 (DJCLS R15/20) and the Interdisziplinäres Zentrum für Klinische Forschung (IZKF,
396 Jena, Germany).

397 **Conflict of Interest**

398 The authors declare no conflict of interest.

399 **References**

- 400 1 Shtivelman E, Lifshitz B, Gale RP, Canaani E. Fused transcript of abl and bcr
401 genes in chronic myelogenous leukaemia. *Nature* 1985; 315(6020):550-4.
- 402 2 James C, Ugo V, Le Couédic JP, Staerk J, Delhommeau F, Lacout C et al. A
403 unique clonal JAK2 mutation leading to constitutive signalling causes
404 polycythaemia vera. *Nature* 2005; 434(7037):1144-8.
- 405 3 Vardiman JW, Thiele J, Arber DA, Brunning RD, Borowitz MJ, Porwit A *et al.*
406 The 2008 revision of the World Health Organization (WHO) classification of
407 myeloid neoplasms and acute leukemia: rationale and important changes.
408 *Blood* 2009; 114:937-51.
- 409 4 Druker BJ, Tamura S, Buchdunger E, Ohno S, Segal GM, Fanning S et al.
410 Effects of a selective inhibitor of the Abl tyrosine kinase on the growth of Bcr-
411 Abl positive cells. *Nature Medicine* 1996; 2(5):561-6.
- 412 5 Zoi K, Cross NC. Molecular pathogenesis of atypical CML, CMML and
413 MDS/MPN-unclassifiable. *International Journal of Hematology* 2015;
414 101(3):229-42.
- 415 6 Shih AH, Abdel-Wahab O, Patel JP, Levine RL. The role of mutations in
416 epigenetic regulators in myeloid malignancies. *Nature Reviews Cancer* 2012;
417 12(9):599-612.

- 418 7 Kon A, Shih LY, Minamino M, Sanada M, Shiraishi Y, Nagata Y et al.
419 Recurrent mutations in multiple components of the cohesin complex in myeloid
420 neoplasms. *Nature Genetics* 2013; 45(10):1232-7.
- 421 8 Yoshida K, Sanada M, Shiraishi Y, Nowak D, Nagata Y, Yamamoto R et al.
422 Frequent pathway mutations of splicing machinery in myelodysplasia. *Nature*
423 2011; 478(7367):64-9.
- 424 9 Fathi AT, Abdel-Wahab O. Mutations in epigenetic modifiers in myeloid
425 malignancies and the prospect of novel epigenetic-targeted therapy. *Advances*
426 *in Hematology* 2012; 2012:469592.
- 427 10 Kim KH, Roberts CW. Targeting EZH2 in cancer. *Nature Medicine* 2016;
428 22(2):128-34.
- 429 11 Ernst T, Chase AJ, Score J, Hidalgo-Curtis CE, Bryant C, Jones AV et al.
430 Inactivating mutations of the histone methyltransferase gene EZH2 in myeloid
431 disorders. *Nature Genetics* 2010; 42(8):722-6.
- 432 12 Chomczynski P, Sacchi N. Single-step method of RNA isolation by acid
433 guanidinium thiocyanate-phenol-chloroform extraction. *Analytical Biochemistry*
434 1987; 162(1):156-9.
- 435 13 Schäfer V, Ernst J, Rinke J, Ziermann J, Winkelmann N, Hochhaus A et al.
436 EZH2 mutations and promoter hypermethylation in childhood acute
437 lymphoblastic leukemia. *Journal of Cancer Research and Clinical Oncology*
438 2016; 142(7):1641-50.
- 439 14 Rinke J, Schäfer V, Schmidt M, Ziermann J, Kohlmann A, Hochhaus A et al.
440 Genotyping of 25 leukemia-associated genes in a single work flow by next-
441 generation sequencing technology with low amounts of input template DNA.
442 *Clinical Chemistry* 2013; 59(8):1238-50.

- 443 15 Schmidt M, Rinke J, Schäfer V, Schnittger S, Kohlmann A, Obstfelder E et al.
444 Molecular-defined clonal evolution in patients with chronic myeloid leukemia
445 independent of the *BCR-ABL* status. *Leukemia* 2014; 28(12): 2292-9.
- 446 16 Sauer H, Ruhe C, Müller JP, Schmelter M, D'Souza R, Wartenberg M.
447 Reactive oxygen species and upregulation of NADPH oxidases in
448 mechanotransduction of embryonic stem cells. *Methods in Molecular Biology*
449 2008; 477:397-418.
- 450 17 Rittirsch D, Schoenborn V, Lindig S, Wanner E, Sprengel K, Günkel S et al. An
451 Integrated Clinico-transcriptomic Approach Identifies a Central Role of the
452 Heme Degradation Pathway for Septic Complications after Trauma. *Annals of*
453 *Surgery* 2016; 264(6):1125-1134.
- 454 18 Zirm E, Spies-Weisshart B, Heidel F, Schnetzke U, Böhmer FD, Hochhaus A
455 et al. Ponatinib may overcome resistance of FLT3-ITD harbouring additional
456 point mutations, notably the previously refractory F691I mutation. *British*
457 *Journal of Haematology* 2012; 157(4):483-92.
- 458 19 Khan SN, Jankowska AM, Mahfouz R, Dunbar AJ, Sugimoto Y, Hosono N et
459 al. Multiple mechanisms deregulate EZH2 and histone H3 lysine 27 epigenetic
460 changes in myeloid malignancies. *Leukemia* 2013; 27(6):1301-9.
- 461 20 Papaemmanuil E, Gerstung M, Malcovati L, Tauro S, Gundem G, Van Loo P
462 et al. Clinical and biological implications of driver mutations in myelodysplastic
463 syndromes. *Blood* 2013; 122(22):3616-27
- 464 21 Bejar R, Stevenson KE, Caughey BA, Abdel-Wahab O, Steensma DP, Galili N
465 et al. Validation of a prognostic model and the impact of mutations in patients
466 with lower-risk myelodysplastic syndromes. *Journal of Clinical Oncology* 2012;
467 30(27):3376-82.

- 468 22 Murati A, Brecqueville M, Devillier R, Mozziconacci MJ, Gelsi-Boyer V,
469 Birnbaum D. Myeloid malignancies: mutations, models and management.
470 *BMC Cancer* 2012; 12:304.
- 471 23 Abdel-Wahab O, Adli M, LaFave LM, Gao J, Hricik T, Shih AH et al. ASXL1
472 mutations promote myeloid transformation through loss of PRC2-mediated
473 gene repression. *Cancer Cell* 2012; 22(2):180-93.
- 474 24 Itzykson R, Kosmider O, Renneville A, Morabito M, Preudhomme C, Berthon C
475 et al. Clonal architecture of chronic myelomonocytic leukemias. *Blood* 2013;
476 121(12):2186-98.
- 477 25 Anderson K, Lutz C, van Delft FW, Bateman CM, Guo Y, Colman SM et al.
478 Genetic variegation of clonal architecture and propagating cells in leukaemia.
479 *Nature* 2011; 469(7330):356-61.
- 480 26 Mason CC, Khorashad JS, Tantravahi SK, Kelley TW, Zabriskie MS, Yan D et
481 al. Age-related mutations and chronic myelomonocytic leukemia. *Leukemia*
482 2016; 30(4):906-13.
- 483 27 Jankowska AM, Makishima H, Tiu RV, Szpurka H, Huang Y, Traina F et al.
484 Mutational spectrum analysis of chronic myelomonocytic leukemia includes
485 genes associated with epigenetic regulation: UTX, EZH2, and DNMT3A. *Blood*
486 2011; 118(14):3932-41.
- 487 28 Kühnl A, Valk PJ, Sanders MA, Ivey A, Hills RK, Mills KI et al. Downregulation
488 of the Wnt inhibitor CXXC5 predicts a better prognosis in acute myeloid
489 leukemia. *Blood* 2015; 125(19):2985-94.
- 490 29 Seth A, Watson DK. ETS transcription factors and their emerging roles in
491 human cancer. *European Journal of Cancer* 2005; 41(16):2462-78.

- 492 30 Collyn d'Hooghe M, Galiègue-Zouitina S, Szymiczek D, Lantoine D, Quief S,
493 Loucheux-Lefebvre MH et al. Quantitative and qualitative variation of ETS-1
494 transcripts in hematologic malignancies. *Leukemia* 1993; 7(11):1777-85.
- 495 31 Kerckaert JP, Duterque-Coquillaud M, Collyn-d'Hooghe M, Morel P, Majérus
496 MA, Laï JL et al. Polymorphism of the proto-oncogene ETS-1 in hematological
497 malignancies. *Leukemia* 1990; 4(1):16-9.
- 498 32 Nowak D, Le Toriellec E, Stern MH, Kawamata N, Akagi T, Dyer MJ et al.
499 Molecular allelokaryotyping of T-cell prolymphocytic leukemia cells with high
500 density single nucleotide polymorphism arrays identifies novel common
501 genomic lesions and acquired uniparental disomy. *Haematologica* 2009;
502 94(4):518-27.
- 503 33 del Rey M, O'Hagan K, Dellett M, Aibar S, Colyer HA, Alonso ME et al.
504 Genome-wide profiling of methylation identifies novel targets with aberrant
505 hypermethylation and reduced expression in low-risk myelodysplastic
506 syndromes. *Leukemia* 2013; 27(3):610-8.
- 507 34 Goyama S, Schibler J, Gasilina A, Shrestha M, Lin S, Link KA et al.
508 UBASH3B/Sts-1-CBL axis regulates myeloid proliferation in human
509 preleukemia induced by AML1-ETO. *Leukemia* 2016; 30(3):728-39.
- 510 35 Hobert O, Jallal B, Ullrich A. Interaction of Vav with ENX-1, a putative
511 transcriptional regulator of homeobox gene expression. *Molecular Cell Biology*
512 1996; 16(6):3066-73.
- 513 36 Fujikawa K, Miletic AV, Alt FW, Faccio R, Brown T, Hoog J et al. Vav1/2/3-null
514 mice define an essential role for Vav family proteins in lymphocyte
515 development and activation but a differential requirement in MAPK signaling in
516 T and B cells. *The Journal of Experimental Medicine* 2003; 198(10):1595-608.

- 517 37 Chang KH, Sanchez-Aguilera A, Shen S, Sengupta A, Madhu MN, Ficker AM
518 et al. Vav3 collaborates with p190-BCR-ABL in lymphoid progenitor
519 leukemogenesis, proliferation, and survival. *Blood* 2012; 120(4):800-11.
- 520 38 Viré E, Brenner C, Deplus R, Blanchon L, Fraga M, Didelot C et al. The
521 Polycomb group protein EZH2 directly controls DNA methylation. *Nature* 2006;
522 439(7078):871-4. Erratum in: *Nature* 2007; 446(7137):824.

523

524 **Figure legends**

525 **Figure 1** *Cooperation of distinct and individual mutations detected by NGS in a*
526 *cohort of 41 EZH2-positive MDS/MPN patients. A total of 190 individual mutations*
527 *were detected. Patients carried between 1 and 9 mutations of up to 7 different genes.*
528 ** frameshift, nonsense and/or splice donor/acceptor mutation(s); ⁰ two detected*
529 *mutations; ~ three detected mutations. Detailed information is given in Supplemental*
530 *Table 4. Patient information such as karyotype and diagnostic category can be*
531 *viewed in Supplemental Table 1.*

532 **Figure 2** *Clonal branching and mutational frequencies detected in patients #24, 37,*
533 *40 and 41. Putative evolutionary trees generated from targeted analysis of CFU-GM*
534 *derived colonies from CD34+ cells, accounting for the zygosity status at each locus*
535 *(italicized: heterozygous, bold & underlined: homozygous). Only mutated genes are*
536 *indicated in each subclone. (A) Patient #40: Analysis of 80 individual colonies for*
537 *mutations previously detected by NGS, indicate initial *EZH2* mutation followed by*
538 **SETBP1* and *CBL* mutations. The dominant clone (78%) is homozygous for both*
539 **EZH2* and *CBL* and heterozygous for *SETBP1*, branching of into clones that carry*
540 *either wild type (6%) or homozygous (4%) *SETBP1* alleles. (B) Patient #37: Analysis*
541 *of 49 colonies showing initial homozygous *EZH2* mutation followed by *SETBP1* and*
542 **NRAS* mutations. The dominant clone (49%) is homozygous for *EZH2* and*

543 heterozygous for *SETBP1* and *NRAS*, branching of into clones that are either
544 homozygous for *SETBP1* (10%) or *NRAS* (20%) and finally, a clone homozygous for
545 all said mutations. Low-level *KRAS*, *RUNX1*, *STAG2* and *ZRSR2* mutations
546 previously identified by NGS were not detected in colonies. (C) Patient #24: Analysis
547 of 41 colonies indicates an initial heterozygous *EZH2* and *SETBP1* positive clone,
548 followed by the acquisition of heterozygous *CBL* and *SRSF2* mutations and finally
549 *STAG2*, which is homozygous in the dominant clone (54%). The complex pattern of
550 mutations shows allele losses at all loci, with reversion to homozygous and/or wild-
551 type state. (D) Patient #41: Analysis of 46 colonies indicates the early acquisition of
552 an *ASXL1* mutation, followed by *EZH2* mutations p.T467Hfs*16 and p.Y579X,
553 respectively, with frequent allele loss. The dominant clone (35%) is heterozygous for
554 all mutations.

555 **Figure 3** Whole transcriptome analysis of *EZH2*-wild type and mutant MDS/MPN
556 patients ($n = 12$, each). (A) Cloud diagram of average signal intensities detected for
557 34,694 genes in *EZH2*-wild type and mutant patients shows distinct differences in
558 gene expression for genes with signal intensities above ~ 5000 . (B) Correlation
559 Cluster analysis (hierarchical clustering; nesting with average linking method;
560 Pearson correlation using 1-r distance measure) of patient data and heat map
561 showing ≥ 2 FC differently expressed genes and background corrected average
562 signal intensities > 200 . Clustered columns, sorted by average signal of wild type
563 group. Patients #34 and A did not match the gene expression pattern of their
564 respective group. The majority of genes show upregulated expression levels in the
565 *EZH2*-wild type group. (C) Microarray average signal intensities and Log2 data of
566 known *EZH2* targets *ADRB2*, *JAK1*, *JAK2* and *MYC* for *EZH2*-wild type and mutant
567 patients; (*) $p \leq 0.05$; (**) $p \leq 0.005$. Detailed information is given in Supplemental Table
568 4.

569 **Figure 4** *Microarray and qRT-PCR expression data of genes regulated in both*
570 *patients and cell lines in relation to EZH2-aberration.* Genes showing differences
571 between patients depending on *EZH2* status in comparison to cell line data; (*)
572 $p \leq 0.05$; (**) $p \leq 0.005$; (***) $p \leq 0.0005$; Mean and standard deviation of microarray
573 average signal intensities and Log2 expression ratios of (i) Microarray and (ii) qRT-
574 PCR data (A) Expression data of genes with significant ≥ 2 FC differences between
575 *EZH2*-wild type and mutant patients (n = 12, each); (B) Expression data of genes
576 with significant differences between control and shRNA manipulated F-36P cell lines
577 (n = 4, each); (C) Expression data of genes with significant differences between
578 control and shRNA manipulated MOLM-13 cell lines (n = 4, each); (D) Expression
579 data of genes with significant differences between control and shRNA manipulated
580 OCI-M2 cell lines (n = 4, each). Differences between microarray and qRT-PCR data
581 are due to inter-assay variations. Detailed information is given in Supplemental Table
582 4.

583 **Figure 5** *Protein blot analysis of F-36P, MOLM-13, OCI-M2 and patient data.* Cell
584 lines expressing *EZH2*-targeting shRNA genes 1 or 2 (sh 1, sh 2) or a nontargeting
585 control shRNA and patient cell samples were lysed and processed via SDS-PAGE
586 and immunoblotted. Histone H3 and GAPDH were used as loading controls. (A)
587 Protein blots show a reduced *EZH2* expression in manipulated cells as well as a
588 reduced H3K27 trimethylation. ETS-1, STS-1 and VAV3 show upregulation in
589 manipulated cell lines. Marginal downregulation was observed for CXXC5 and
590 FAM113B for all cell lines. (B) Cell line protein blots, semi-quantified using H3 as a
591 reference for H3K27me3 and GAPDH as a reference for all other proteins (C) Protein
592 blots of *EZH2*-mutant patients #24 (p.N263Qfs*8), 27 (p.K685Rfs*12), 32
593 (p.K17Sfs*3) and 34 (p.Y292X) show a reduced *EZH2* expression, particularly for

594 homozygous patients #27 and 32, and a reduced H3K27me3 expression, compared
595 to *EZH2*-wild type patients D and F.

Figure 2A

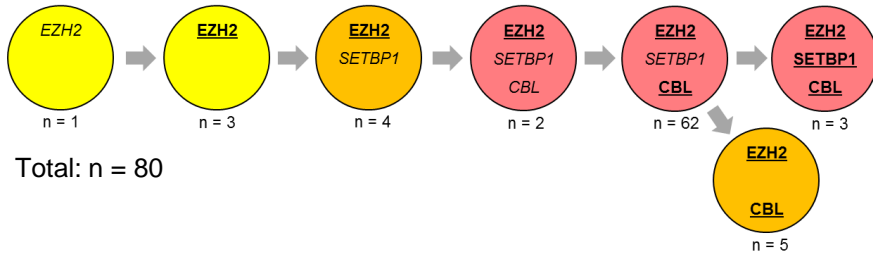


Figure 2B

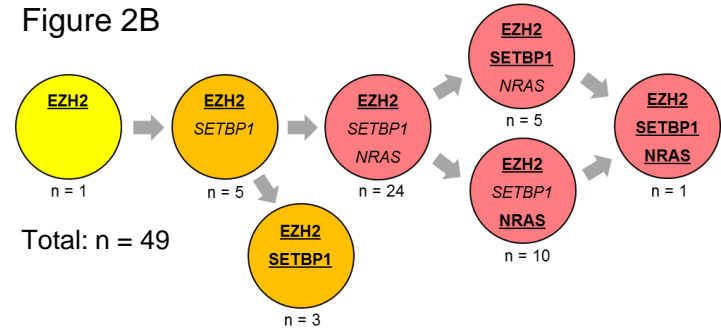


Figure 2C

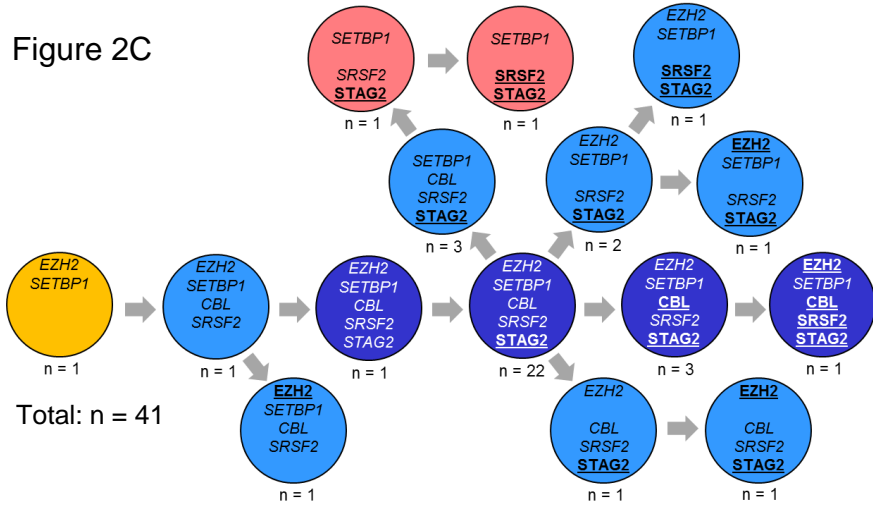
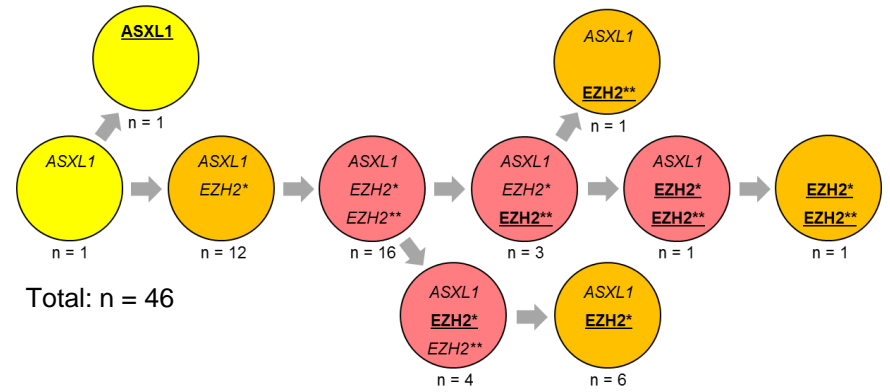


Figure 2D



Legend

- 1 Mutation/colony
- 2 Mutations/colony
- 3 Mutations/colony
- 4 Mutations/colony
- 5 Mutations/colony
- K Heterozygous mutation
- B Homozygous mutation

Figure 3A

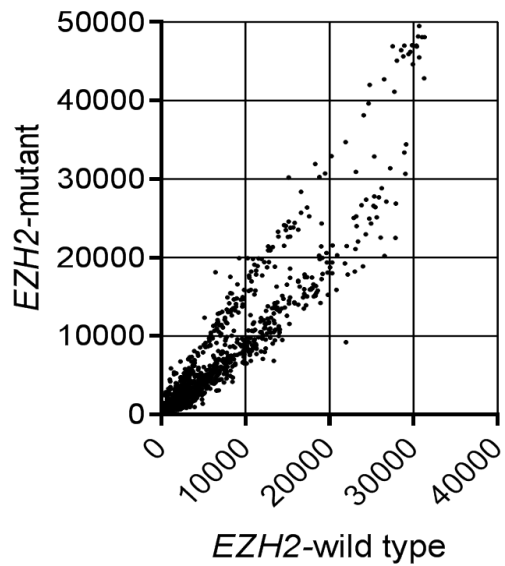


Figure 3B

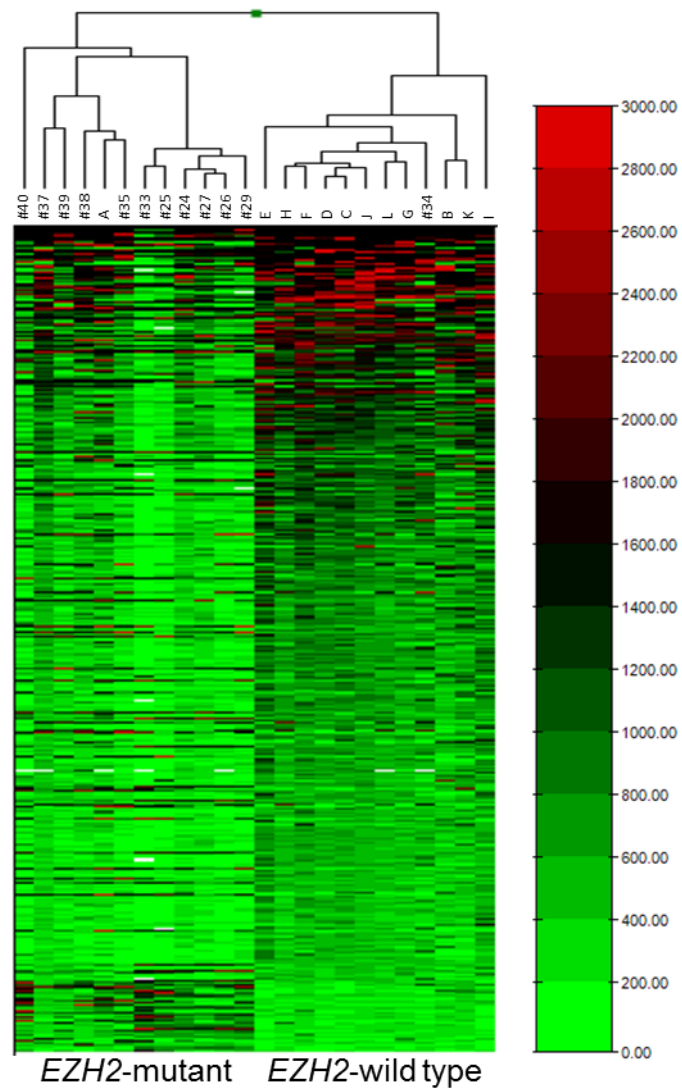


Figure 3C

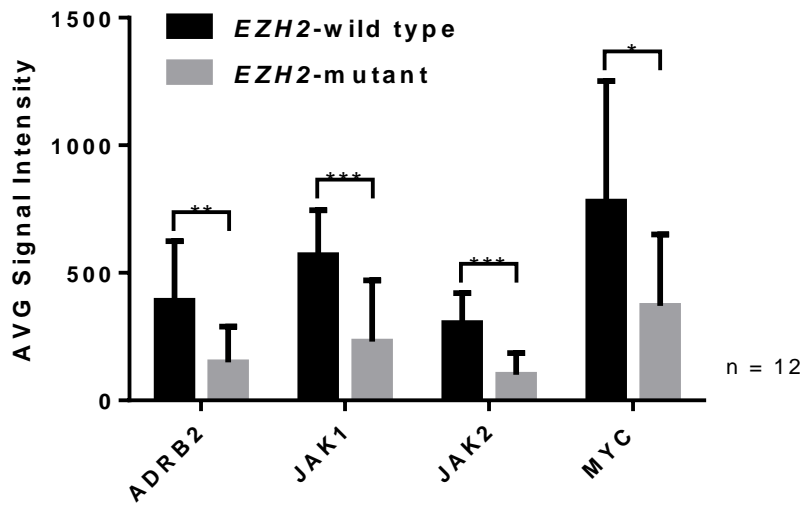


Figure 4A

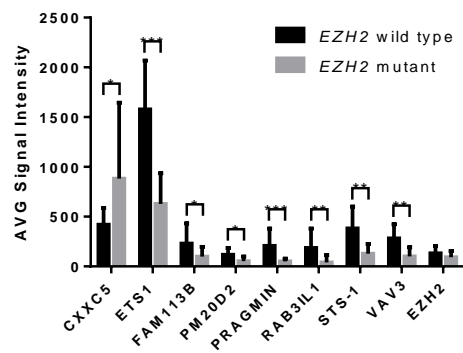


Figure 4B

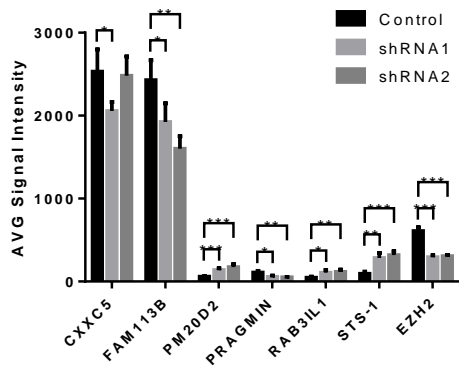


Figure 4C

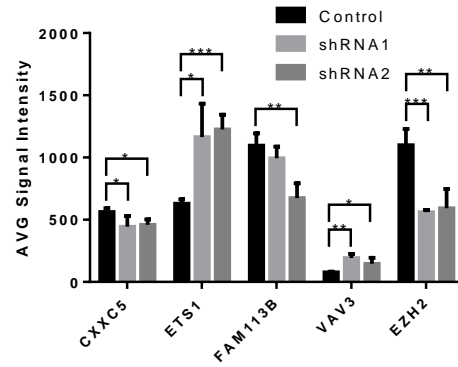
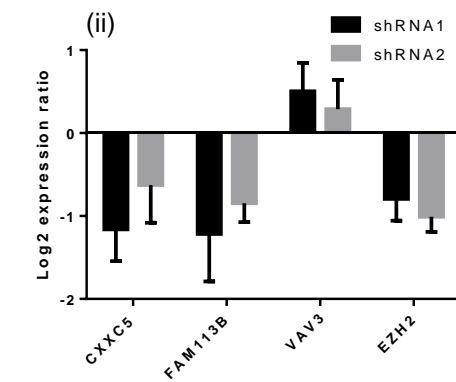
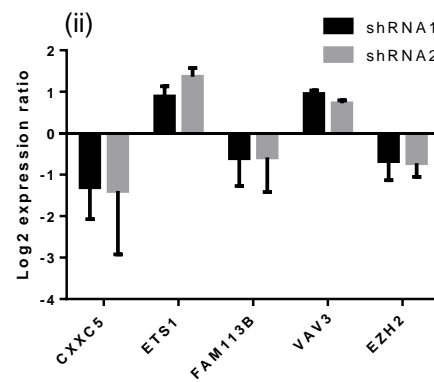
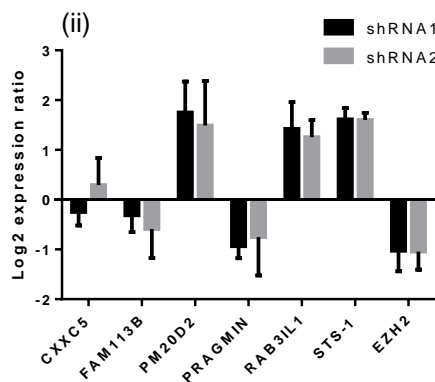
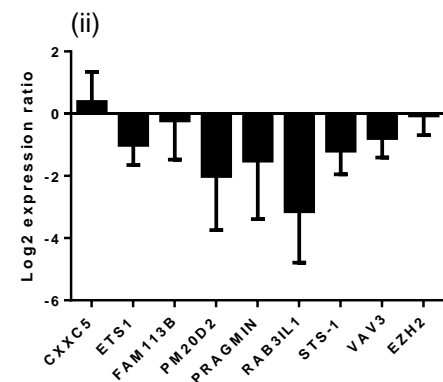
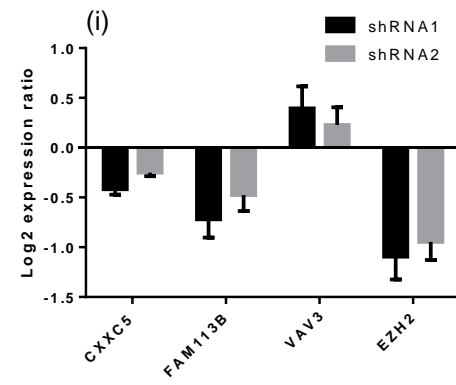
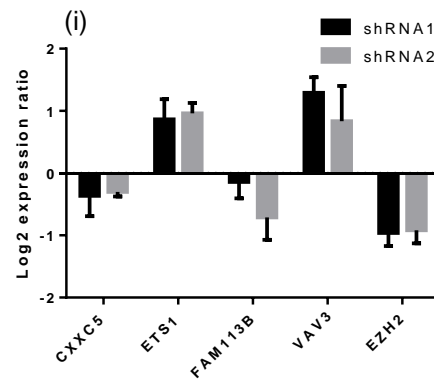
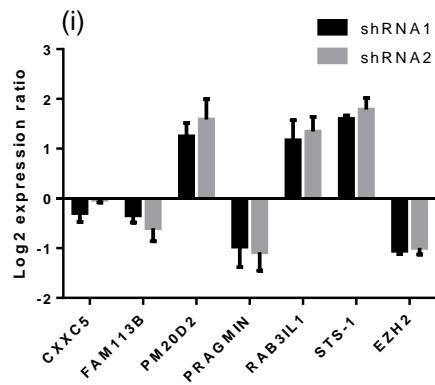
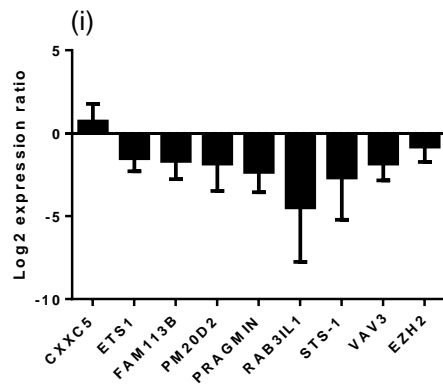
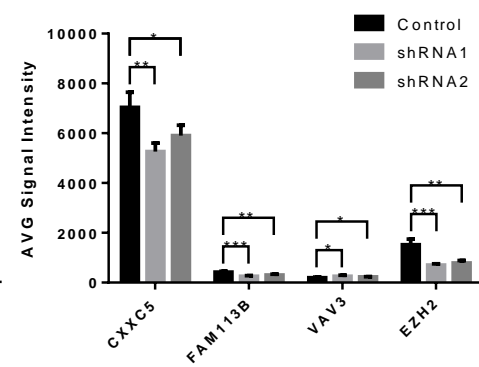


Figure 4D



Patients

F-36P

MOLM-13

OCI-M2

